Monthly Notices
of the
ROYAL ASTRONOMICAL SOCIETY

Mon. Not. R. Astron. Soc. **420,** 2034–2041 (2012) doi:10.1111/j.1365-2966.2011.20144.x

Dwarf spheroidal galaxy kinematics and spiral galaxy scaling laws

Paolo Salucci,[1] Mark I. Wilkinson,[2] Matthew G. Walker,[3]★ Gerard F. Gilmore,[4] Eva K. Grebel,[5] Andreas Koch,[6] Christiane Frigerio Martins[7]† and Rosemary F. G. Wyse[8]

[1]*Department of Astrophysics, SISSA, Via Beirut, 2-4, 34014 Trieste, Italy*
[2]*Department of Physics and Astronomy, University of Leicester, University Road, Leicester LE1 7RH*
[3]*Harvard-Smithsonian Center for Astrophysics, 60 Garden Street, Cambridge, MA 02138, USA*
[4]*Institute of Astronomy, University of Cambridge, Madingley Road, Cambridge CB3 OHA*
[5]*Astronomisches Rechen-Institut, Zentrum für Astronomie der Universität Heidelberg, Mönchhofstr. 12-14, 69120 Heidelberg, Germany*
[6]*Zentrum für Astronomie der Universität Heidelberg, Landessternwarte, Königstuhl 12, 69117 Heidelberg, Germany*
[7]*INFES, Universidade Federal Fluminense, av. João Jazbik. 28470 Santo Antônio de Pádua, Rio de Janeiro, Brazil*
[8]*Department of Physics and Astronomy, Johns Hopkins University, 3400 N. Charles Street, 21218-2686 Baltimore, MD, USA*

Accepted 2011 November 4. Received 2011 November 3; in original form 2011 October 15

ABSTRACT

Kinematic surveys of the dwarf spheroidal (dSph) satellites of the Milky Way are revealing tantalizing hints about the structure of dark matter (DM) haloes at the low-mass end of the galaxy luminosity function. At the bright end, modelling of spiral galaxies has shown that their rotation curves are consistent with the hypothesis of a universal rotation curve whose shape is supported by a cored dark matter halo. In this paper, we investigate whether the internal kinematics of the Milky Way dSphs are consistent with the particular cored DM distributions which reproduce the properties of spiral galaxies. Although the DM densities in dSphs are typically almost two orders of magnitude higher than those found in (larger) disc systems, we find consistency between dSph kinematics and Burkert DM haloes whose core radii r_0 and central densities ρ_0 lie on the extrapolation of the scaling law seen in spiral galaxies: $\log\ \rho_0 \simeq \alpha\ \log\ r_0 + \text{const}$ with $0.9 < \alpha < 1.1$. We similarly find that the dSph data are consistent with the relation between ρ_0 and baryon scalelength seen in spiral galaxies. While the origin of these scaling relations is unclear, the finding that a single DM halo profile is consistent with kinematic data in galaxies of widely varying size, luminosity and Hubble type is important for our understanding of observed galaxies and must be accounted for in models of galaxy formation.

Key words: galaxies: dwarf – galaxies: kinematics and dynamics – Local Group – dark matter.

1 INTRODUCTION

In the current cosmological paradigm, dark matter (DM) provides the gravitational potential wells in which galaxies form and evolve. Over the past few decades, observations have provided detailed information about the distribution of DM within those regions of spiral galaxies where the baryons reside [Ashman 1992; Persic, Salucci & Stel 1996 (hereafter PSS); Sofue & Rubin 2001; Salucci et al. 2007]. Similar information on the distribution of DM is also available for low-surface-brightness (LSB) galaxies (de Blok 2005; Kuzio de Naray et al. 2006). In these disc systems, the ordered rotational motions and known geometry of the tracers have facilitated the mass modelling and provided clear evidence that the stellar components of spiral galaxies are embedded in extended DM haloes. In the most luminous objects, the stellar disc is almost self-gravitating with DM contributing significantly to the dynamics only at larger radii. In contrast, at the faint end of the galaxy luminosity function, baryons contribute a negligible amount to the overall gravitational potential (de Blok et al. 2008).

Extensive modelling of both individual and co-added spiral galaxy rotation curves (RCs) has generally concluded that almost maximal stellar discs embedded in cored DM haloes reproduce the data better than models with cosmologically motivated, cusped DM haloes (PSS; Salucci & Burkert 2000; de Blok, McGaugh & Rubin 2001; de Blok & Bosma 2002; Marchesini 2002; Gentile et al. 2004, 2005, 2007; see also Chemin, de Blok & Mamon 2011).

★Hubble fellow.
†E-mail: cfrigerio@ufabc.edu.br

Furthermore, scaling relations between properties of the spiral galaxies such as central surface density, stellar scale radius and stellar velocity dispersion have been identified and interpreted as signatures of the physical processes which drive galaxy formation (e.g. Kormendy 1985, 1987, 1990; Burkert 1995; Kormendy & Freeman 2004).

Persic & Salucci (1988, 1991)) demonstrated that the Burkert halo density profile given by

$$\rho(r) = \frac{\rho_0\, r_0^3}{(r + r_0)\,\left(r^2 + r_0^2\right)}, \qquad (1)$$

with two free parameters, the core radius r_0 and the central halo density ρ_0, is consistent with the available kinematic data in spiral galaxies. When the mass distribution in these galaxies is modelled using the combined contributions of a Freeman (1970) disc for the luminous matter and a Burkert profile for the DM halo, the structural parameters obtained (DM central densities, core radii, disc masses and length-scales) exhibit a series of scaling laws. This led to the hypothesis of a 'universal rotation curve' (URC), an empirical function of radius and luminosity that reproduces the RCs of spiral galaxies (Persic & Salucci 1988, 1991; PSS; Salucci et al. 2007 and references therein).

In contrast, our knowledge of the mass distribution in pressure-supported systems such as elliptical galaxies is still limited (see Napolitano, Romanowsky & Tortora 2010 for a recent summary of the state of the art). Ongoing observations of Local Group dwarf spheroidal galaxies (dSphs), which occupy the faint end of the luminosity function of pressure-supported systems, are currently yielding crucial information about the properties of the dark and luminous components in these objects and, in turn, on the underlying physical properties of DM haloes (e.g. Tolstoy et al. 2004; Gilmore et al. 2007; Peñarrubia, McConnachie & Navarro 2008; Strigari et al. 2008; Walker, Mateo & Olszewski 2009a). It is, however, an intrinsically difficult task both observationally, in terms of measuring velocities for sufficient numbers of tracers, and from a dynamical modelling point of view, due the lack of precise information on the dynamical state of the stellar populations.

The dSphs are typically at least two orders of magnitude less luminous than the faintest spirals, and show evidence of being DM dominated at all radii (e.g. Kleyna et al. 2002). Their typical stellar masses lie in the range of 3×10^5 to $2 \times 10^7\,\mathrm{M}_\odot$, although the luminous masses of some recently discovered objects are as low as $10^3\,\mathrm{M}_\odot$ (Martin, de Jong & Rix 2008), while their stellar length-scales are of the order of 0.3 kpc. In these systems, the DM halo typically outweighs the baryonic matter by a large factor (from a few tens, up to several hundred). An understanding of these objects is therefore essential for understanding the nature of dark matter itself and to build an observational picture of the outcome of galaxy formation on small scales. Additionally, high-redshift dSph precursors most likely contributed significantly to the build-up of the stellar halo of the Milky Way (Helmi 2008). Given that the observed dSphs are predominantly old, pressure-supported, spheroidal systems, their evolutionary histories would be expected to differ significantly from those of spirals, especially in the baryonic components (see e.g. Grebel, Gallagher & Harbeck 2003).

As in the case of spiral galaxies, a number of authors have found evidence of universality in the DM halo properties of dSph galaxies. Mateo (1998) found that the variation of the mass-to-light ratios of dSphs with total luminosity was consistent with all dSphs containing similar masses of dark matter within the volume occupied by their stellar distributions. This implies a larger proportion of dark matter in the less luminous objects, a general characteristic of spiral galaxy haloes (Persic & Salucci 1988; de Blok et al. 2008). More recent analyses (Gilmore et al. 2007; Koch et al. 2007a; Strigari et al. 2008; Walker et al. 2009b), based on extended velocity dispersion profiles rather than central velocity dispersions alone, have generally supported this conclusion.

A number of important questions remain unanswered. First, is the distribution of DM on galactic (i.e. kpc) scales really universal? For example, Adén et al. (2009) have noted the existence of considerable scatter in the estimated masses of the lowest luminosity systems, and several authors have presented evidence of systematic differences between the properties of the Milky Way dSph satellites and those surrounding M31 (Collins et al. 2010, 2011; Kalirai et al. 2010). Secondly, why do the properties of the dark and luminous mass distributions appear to be related, even though baryons dominate, at most, only the inner regions of galaxies?

The study of the internal kinematics of the Milky Way dSphs has been revolutionized by the availability of multi-object spectrographs on 4-m and 8-m-class telescopes. Large data sets comprising between several hundred and several thousand individual stellar velocities per galaxy have now been acquired for all the luminous dSphs surrounding the Milky Way (Kleyna et al. 2004; Wilkinson et al. 2004; Muñoz et al. 2005, 2006; Koch et al. 2007a,b; Battaglia et al. 2008; Walker et al. 2009a). The volume of the currently available data is sufficient to measure the dynamical masses interior to the stellar distributions of the dSphs. However, the mass profiles remain less well determined. It has been demonstrated (Koch et al. 2007a,b; Walker et al. 2007; Battaglia et al. 2008) that these profiles are consistent with the cuspy dark matter haloes produced in cosmological *N*-body simulations (e.g. Navarro, Frenk & White 1997), as well as with more general families of haloes that range from centrally cored to steeply cusped (Walker et al. 2009b). The velocity dispersion profiles alone cannot distinguish between cored and cusped haloes due to the degeneracy between mass and velocity anisotropy (see e.g. Koch et al. 2007a; Battaglia et al. 2008; Evans, An & Walker 2009). Gilmore et al. (2007) recently showed that the kinematic data and additional features in a small number of the well-studied dSphs are consistent with cored DM potentials, under the assumptions of spherical symmetry and velocity isotropy. In addition, several authors have presented arguments which suggest that the internal kinematics of dSphs may be more consistent with cored haloes (Kleyna et al. 2002; Goerdt et al. 2006; Battaglia et al. 2008; Walker & Peñarrubia 2011; Amorisco & Evans 2012).

In the present paper, we investigate whether DM haloes of Burkert form are consistent with the observed kinematics of the luminous Milky Way dSphs. As noted above, Burkert haloes provide good matches to the rotation curves of spiral galaxies and it is therefore interesting to ask whether they are also relevant models for galaxies of other Hubble types. We also wish to explore whether the parameters of the best-fitting Burkert profiles for the dSphs lie on the extrapolation to the dSph regime of the scaling relations seen in spiral galaxies. While previous work has already shown that the internal kinematics of the Milky Way dSphs may be consistent with cored haloes (Gilmore et al. 2007), it does not necessarily follow that Burkert profiles in particular reproduce the observed kinematic data.

In what follows, we assume that the form of the dSph dark matter halo density is known and only the length-scale and density scale can vary. We allow the velocity anisotropy of the stellar distribution to vary in order to reproduce the observed dispersion profiles as closely as possible. Finally, we compare the resulting DM structural parameters with the low-luminosity extrapolation of the relations between the equivalent parameters found in spirals.

Some of the comparisons between dSphs and spirals require us to define a stellar length-scale for the dSphs which plays the same role as the disc scalelength R_D in spirals. One way to do this is to identify the location of the peak in the circular velocity curves in each system which would be predicted if the stellar components were assumed to contribute all the gravitating mass. For a Freeman disc, this peak occurs at 2.2 R_D. If the stellar components of the dSphs are modelled using a Plummer (1915) sphere, the corresponding radius is at $1.4r_h$ (r_h is the projected half-light radius). Thus, where necessary, we associate the spiral disc length-scale R_D with the radius $0.64r_h$ in the dSphs. However, we note that most of our conclusions in this paper do not make use of this length-scale.

The outline of the paper is as follows. In Section 2, we summarize the observational data used in our study and describe in detail the analysis of the dSph data. Section 3 compares the properties of the dark haloes of spiral and dSph galaxies. Section 4 summarizes our findings and speculates on their implications for our understanding of dark matter and galaxy formation.

2 DATA

2.1 dSph galaxies

Fig. 1 displays empirical velocity dispersion profiles originally published by Walker et al. (2007, 2009a,b) and Mateo, Olszewski & Walker (2008) for the Milky Way's 'classical" dSph satellites Carina, Draco, Fornax, Leo I, Leo II, Sculptor, Sextans and Ursa Minor. As discussed above, in our present analysis, we assume Burkert profiles for the dark matter haloes of the dSphs in order to provide a basis for comparison with spiral galaxies. Specifically, we use the previously published velocity dispersion profiles shown in Fig. 1 to constrain values of the Burkert parameters ρ_0 and r_0 for each dSph in our sample.

We assume that the luminous component of each dSph consists of a single, pressure-supported stellar population that is in dynamical equilibrium and therefore traces the underlying gravitational potential which we assume to be dominated by the DM halo. The masses of these stellar spheroids can be estimated from their luminosities: they are 1–2 orders of magnitude smaller than the dynamical masses. We assume that the stellar mass-to-light ratios $(M/L)_V$ are unity. While the actual $(M/L)_V$ ratios may vary by about a factor of 2 depending on the details of the stellar populations (see e.g. Mateo et al. 1998), the uncertainties in the modelling results are dominated by the unknown velocity anisotropy.

The Jeans equation relates the density and velocity dispersion of the stellar component to the mass profile of the DM halo. Assuming spherical symmetry, the Jeans equation for a non-rotating system can be written (Binney & Tremaine 2008) as

$$\frac{1}{\nu}\frac{\mathrm{d}}{\mathrm{d}r}\left(\nu\bar{v_r^2}\right) + 2\frac{\beta\bar{v_r^2}}{r} = -\frac{GM(r)}{r^2}, \quad (2)$$

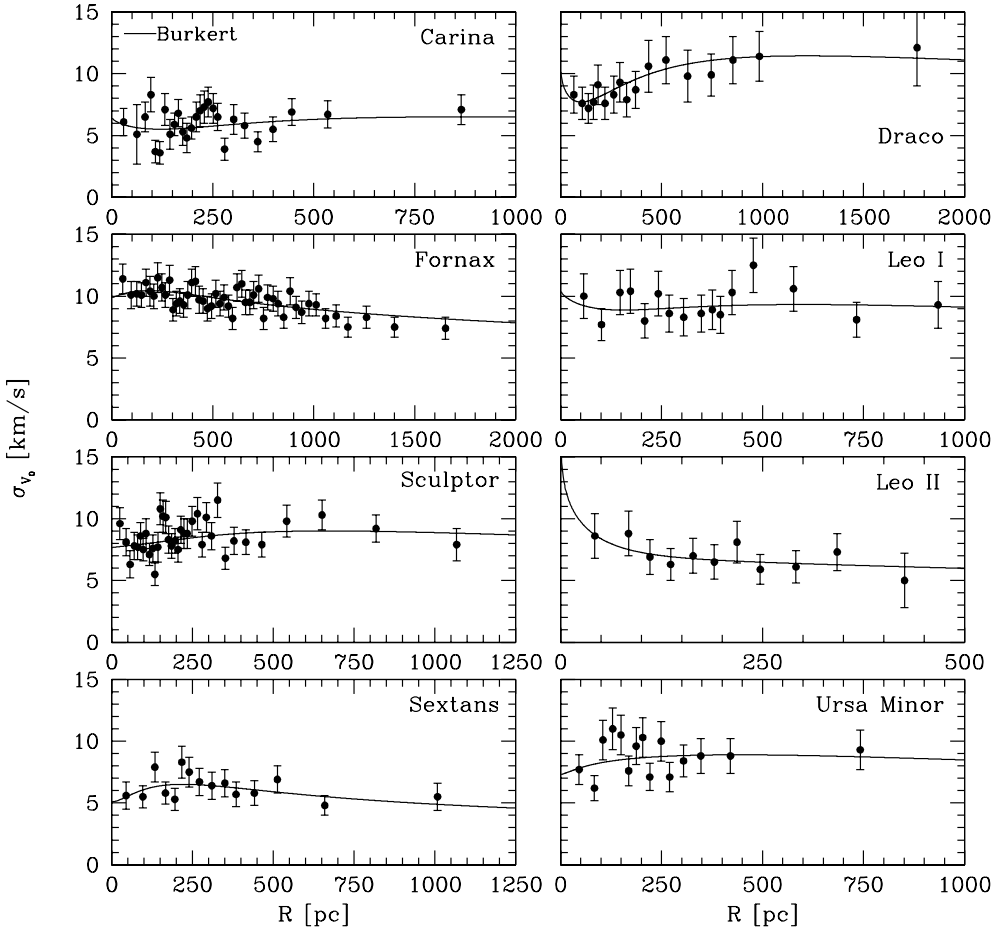

Figure 1. Velocity dispersion profiles for the Milky Way's eight 'classical' dSph satellites. Overplotted are the best-fitting profiles obtained under the assumptions of Burkert DM haloes, Plummer light profiles and radially constant velocity anisotropy. The parameters of each fit, together with associated confidence limits, are listed in Table 1.

where $\nu(r)$, $\bar{v_r^2}(r)$ and $\beta(r) \equiv 1 - \bar{v_\theta^2}/\bar{v_r^2}$ represent the three-dimensional (3D) density, radial velocity dispersion and orbital anisotropy, respectively, of the stellar component, and $M(r)$ is the mass profile of the DM halo. In this analysis, the orbital anisotropy $\beta(r)$ is not constrained, as all information about the velocity distribution is restricted to the component along the line of sight. We make the simplifying assumption that $\beta =$ constant, which provides the following solution to equation (2) (Mamon & Łokas 2005):

$$\nu\bar{v_r^2} = Gr^{-2\beta}\int_r^\infty s^{2\beta-2}\nu(s)M(s)\,\mathrm{d}s. \quad (3)$$

In order to compare to observables, we consider the projection of equation (3) along the line of sight (Binney & Tremaine 2008):

$$\sigma_p^2(R) = \frac{2}{I(R)}\int_R^\infty \left(1-\beta\frac{R^2}{r^2}\right)\frac{\nu\bar{v_r^2}r}{\sqrt{r^2-R^2}}\,\mathrm{d}r, \quad (4)$$

where $I(R)$ is the projected stellar density profile and $\sigma_p(R)$ is the projected velocity dispersion profile. The two parameters of interest are of course the central density and core radius, which enter equation (4) upon substituting for $\nu\bar{v_r^2}$ (equation 3) with the mass profile derived from the Burkert density profile:

$$\begin{aligned} M(r) &= 4\pi\int_0^r s^2\rho(s)\,\mathrm{d}s \\ &= \pi\rho_0 r_0^3\left(\ln\left[(1+r/r_0)^2\left(1+r^2/r_0^2\right)\right] - 2\tan^{-1}[r/r_0]\right). \end{aligned} \quad (5)$$

To describe the stellar density profile, we adopt a Plummer profile, $I(R) = L(\pi r_h^2)^{-1}(1+R^2/r_h^2)^{-2}$, where L is the total luminosity and r_h is the projected half-light radius (i.e. the radius of the circle that encloses half of the total luminosity in projection). Under the assumption of spherical symmetry, the corresponding 3D stellar density is then $\nu(r) = 3L(4\pi r_h^3)^{-1}(1+r^2/r_h^2)^{-5/2}$. Following Walker et al. (2009b), for the eight dSphs considered here, we adopt the V-band luminosities and half-light radii from Irwin & Hatzidimitriou (1995). All values are tabulated in table 1 of Walker et al. (2010).

Treating the stellar density as a known function, we fit halo models to the empirical velocity dispersion profiles using the set of three free parameters: $\boldsymbol{\theta} \equiv \{\theta_1,\theta_2,\theta_3\} = \{\log_{10}[r_0/\mathrm{pc}], \log_{10}[\rho_0/(\mathrm{M}_\odot\,\mathrm{pc}^{-3})], -\log_{10}(1-\beta)\}$. We adopt uniform priors over the ranges $-10 \le \log_{10}[\rho_0/(\mathrm{M}_\odot\,\mathrm{pc}^{-3})] \le 5$, $-2 \le \log_{10}[r_0/\mathrm{pc}] \le 5$ and $-1 \le -\log_{10}(1-\beta) \le 1$. For a given point in parameter space, equation (4) specifies the projected velocity dispersion profile $\sigma_p(R)$. We compare model profiles to the empirical velocity dispersion profiles, $\sigma_{V_0}(R)$ (Fig. 1), by evaluating the likelihood

$$L(\boldsymbol{\theta}) = \prod_{i=1}^{N}\frac{1}{\sqrt{2\pi\mathrm{Var}\left[\sigma_{V_0}^2(R_i)\right]}}\exp\left\{-\frac{1}{2}\frac{\left[\sigma_{V_0}^2(R_i)-\sigma_p^2(R_i)\right]^2}{\mathrm{Var}\left[\sigma_{V_0}^2(R_i)\right]}\right\}, \quad (6)$$

where $\mathrm{Var}[\sigma_{V_0}^2(R_i)]$ is the square of the error associated with the square of the empirical dispersion and N is the number of bins in the dispersion profile. We obtain (marginalized) 1D posterior probability distribution functions for each free parameter using a Markov chain Monte Carlo (MCMC) algorithm. Specifically, we use the same Metropolis–Hastings algorithm (Metropolis et al. 1953; Hastings 1970) described in detail by Walker et al. (2009b). In order to account for the error associated with observational uncertainty in the half-light radius, for each point sampled in our MCMC chains we scatter the adopted value of r_h by a random deviate drawn from a Gaussian distribution with standard deviation equal to the published error (Irwin & Hatzidimitriou 1995). The probability distribution functions for the free parameters are thus effectively marginalized over the range of half-light radii consistent with observations.

Table 1. dSph structural parameters and results of our mass modelling. Columns 1–3: dSph name, observed V-band luminosity and half-light radius (from Irwin & Hatzidimitriou 1995); column 4: velocity anisotropy; columns 5 and 6: density scale and length-scale for the DM halo, assuming a Burkert DM density profile; column 7: halo 'surface density' scale; column 8: total mass interior to $R_{83}/2$, where R_{83} is the radius enclosing 0.83 of the total luminosity; column 9: ratio of stellar mass to DM mass interior to $R_{83}/2$. In columns 4–9, the median value of the parameter is given together with error bars which enclose the central 68 per cent (95 per cent) of the marginalized 1D probability distribution function for the parameter. Since we assume that $M/L_V = 1$ for the stellar components of the dSphs, the luminosities directly yield the stellar masses.

Object	$L_V/L_{V,\odot}$	r_h/pc	$-\log_{10}(1-\beta)$	$\log_{10}[\rho_0/(\mathrm{M}_\odot\,\mathrm{pc}^{-3})]$	$\log_{10}(r_0/\mathrm{pc})$	$\log_{10}[\rho_0 r_0/(\mathrm{M}_\odot\,\mathrm{pc}^{-2})]$	$\log_{10}[M_T(R_{83}/2)/\mathrm{M}_\odot]$	$\log_{10}[M_s(R_{83}/2)/M_h(R_{83}/2)]$
Carina	$(2.4\pm1.0)\times10^5$	241 ± 23	$0.18^{+0.22(+0.47)}_{-0.26(-0.60)}$	$-1.19^{+0.31(+0.75)}_{-0.22(-0.43)}$	$2.78^{+0.28(+0.64)}_{-0.28(-0.59)}$	$1.62^{+0.07(+0.22)}_{-0.05(-0.09)}$	$7.07^{+0.08(+0.12)}_{-0.12(-0.26)}$	$-1.71^{+0.12(+0.27)}_{-0.08(-0.12)}$
Draco	$(2.7\pm0.4)\times10^5$	196 ± 12	$0.26^{+0.35(+0.66)}_{-0.29(-0.76)}$	$-0.74^{+0.22(+0.56)}_{-0.17(-0.30)}$	$2.81^{+0.21(+0.40)}_{-0.23(-0.51)}$	$2.09^{+0.06(+0.14)}_{-0.05(-0.10)}$	$7.31^{+0.09(+0.17)}_{-0.11(-0.20)}$	$-2.17^{+0.11(+0.20)}_{-0.09(-0.17)}$
Fornax	$(1.4\pm0.4)\times10^7$	668 ± 34	$-0.07^{+0.07(+0.14)}_{-0.09(-0.24)}$	$-0.72^{+0.21(+0.57)}_{-0.16(-0.30)}$	$2.57^{+0.09(+0.18)}_{-0.12(-0.30)}$	$1.85^{+0.09(+0.27)}_{-0.07(-0.12)}$	$8.10^{+0.02(+0.03)}_{-0.02(-0.04)}$	$-1.16^{+0.02(+0.04)}_{-0.02(-0.03)}$
Leo I	$(3.4\pm1.1)\times10^6$	246 ± 19	$-0.00^{+0.37(+0.79)}_{-0.47(-0.92)}$	$-0.39^{+0.52(+1.30)}_{-0.35(-0.55)}$	$2.45^{+0.28(+0.51)}_{-0.33(-0.73)}$	$2.07^{+0.18(+0.56)}_{-0.08(-0.13)}$	$7.58^{+0.05(+0.10)}_{-0.07(-0.18)}$	$-1.15^{+0.08(+0.19)}_{-0.06(-0.10)}$
Leo II	$(5.9\pm1.8)\times10^5$	151 ± 17	$-0.15^{+0.71(+1.06)}_{-0.59(-0.81)}$	$0.61^{+2.12(+3.80)}_{-0.92(-1.33)}$	$1.76^{+0.59(+0.96)}_{-0.92(-1.54)}$	$2.39^{+1.18(+2.25)}_{-0.33(-0.47)}$	$7.15^{+0.09(+0.18)}_{-0.09(-0.21)}$	$-1.65^{+0.09(+0.21)}_{-0.10(-0.18)}$
Sculptor	$(1.4\pm0.6)\times10^6$	260 ± 39	$0.01^{+0.11(+0.19)}_{-0.12(-0.25)}$	$-0.61^{+0.16(+0.34)}_{-0.15(-0.27)}$	$2.55^{+0.13(+0.22)}_{-0.11(-0.23)}$	$1.96^{+0.04(+0.10)}_{-0.04(-0.07)}$	$7.55^{+0.03(+0.06)}_{-0.04(-0.10)}$	$-1.48^{+0.04(+0.10)}_{-0.03(-0.06)}$
Sextans	$(4.1\pm1.9)\times10^5$	682 ± 117	$-0.64^{+0.37(+0.60)}_{-0.25(-0.35)}$	$0.74^{+1.39(+3.02)}_{-1.24(-1.97)}$	$1.67^{+0.54(+0.93)}_{-0.55(-1.17)}$	$2.41^{+0.85(+1.87)}_{-0.70(-1.03)}$	$7.51^{+0.09(+0.18)}_{-0.09(-0.17)}$	$-2.09^{+0.09(+0.17)}_{-0.10(-0.18)}$
Ursa Minor	$(2.0\pm0.9)\times10^5$	280 ± 15	$-0.20^{+0.25(+0.50)}_{-0.47(-0.74)}$	$-0.39^{+0.75(+1.39)}_{-0.45(-0.79)}$	$2.39^{+0.36(+0.77)}_{-0.44(-0.74)}$	$2.00^{+0.31(+0.63)}_{-0.09(-0.15)}$	$7.56^{+0.05(+0.09)}_{-0.07(-0.20)}$	$-2.38^{+0.07(+0.20)}_{-0.05(-0.09)}$

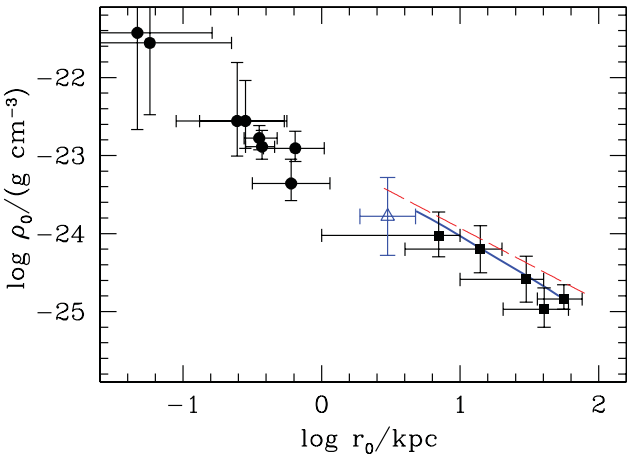

Figure 2. Parameters of Burkert DM haloes obtained from dynamical modelling of (i) spirals, based on the URC hypothesis applied to co-added rotation curves (solid line; data from PSS) or weak-lensing shear (squares; Hoekstra et al. 2005); (ii) NGC 3741 (triangle) the darkest spiral in the local Universe based on its kinematics; (iii) the 'classical' Milky Way dSph satellites (filled circles), based on their internal stellar kinematics (this paper). The Spano et al. (2008) relation is shown as a dashed line.

The velocity dispersion profiles corresponding to the highest-likelihood (equation 6) point from each of our MCMC chains are overplotted on the empirical profiles in Fig. 1. These 'best fits' demonstrate that Burkert profiles can provide an excellent description of dSph velocity dispersion profiles. For each free parameter, we take the 1D posterior probability distribution obtained from our MCMC chains as the observational constraint, given our modelling assumptions. For each free parameter (and combinations thereof), Table 1 identifies the median value and confidence intervals that enclose the central 68 per cent (and 95 per cent) of accepted points in our chains. We find that the dSph haloes have central densities ranging from 7×10^{-24} to 3×10^{-22} g cm^{-3} and core radii ranging from 0.05 to 0.65 kpc. The data in the table also exhibit the well-known mass-anisotropy degeneracy: because the dispersion profiles of the dSphs are essentially flat to large radii and have a relatively small range of amplitudes, larger values of $\rho_0 r_0^3$ are required for galaxies with more radially biased velocity distributions. Our analysis is particularly susceptible to this degeneracy due to our restriction of the modelling to Burkert halo profiles.

We have repeated our analysis with the additional assumption of velocity isotropy (i.e. $\beta = 0$). With the exception of Sextans, the halo parameters obtained for our sample are consistent with those in Table 1 within the quoted uncertainties. When we restrict ourselves to isotropic models, the best-fitting r_0 for Sextans falls to the significantly smaller value of 47 pc. This is consistent with the fact that Sextans is unique in requiring tangential anisotropy to obtain a good fit to the dispersion profile – the best-fitting isotropic model does not match the profile of Sextans interior to 200 pc.

2.2 Spiral galaxies

As discussed above, Burkert halo models provide excellent fits to individual spiral galaxy rotation curves as well as to samples of co-added rotation curves. Moreover, when the mass modelling is performed using Burkert haloes, a tight relation between ρ_0 and r_0 (and also between other parameters like the disc and virial masses) emerges (PSS; Donato, Gentile & Salucci 2004; Salucci et al. 2007). As can be seen in Fig. 2, we find similar ρ_0 versus r_0 relationships *independent* of whether the mass profiles are obtained from rotation curves or from gravitational lensing data and irrespective of whether the analysis is performed on individual or co-added rotation curves.

To emphasize the very different ranges of baryonic mass and extent probed by the dSphs and the spiral galaxies in our sample, in Fig. 3, we compare the relationship between the characteristic baryonic length-scale (R_D; see above for definitions) and the stellar mass of dSphs (estimated from the V-band luminosity, assuming a stellar mass-to-light ratio of unity [in solar units]), and of spirals.

3 DARK MATTER SCALING RELATIONS

In the previous section, we showed that Burkert halo profiles provide good fits to the dSph kinematic data (Fig. 1). In this section, we compare the parameters of the Burkert profiles obtained from our dynamical modelling of dSphs with those obtained for spiral galaxies. In Fig. 2, we plot ρ_0 versus r_0 for the eight dSphs in our sample. Remarkably, they lie on the extrapolation to higher central densities of the relation found for spirals. All these data can be reproduced by the relation $\log\ \rho_0 \simeq \alpha\ \log\ r_0 + \text{const}$ with $0.9 < \alpha < 1.1$.

An even more interesting comparison can be done involving the mean DM surface density within the dark halo core radius (the radius within which the volume density profile of DM remains approximately flat). It was recently discovered (Donato et al. 2009) that this quantity μ_0 ($\mu_0 \equiv \rho_0 r_0$) is constant across a wide range of galaxies of different Hubble type and luminosity and that this relation holds also for dSphs, as we confirm in Fig. 4 , where the data for the dSphs are the results of our Burkert halo modelling in the present paper (in Donato et al. the dSph halo parameters were obtained via a different approach). We therefore confirm that this relation extends across a luminosity range of 14 mag and spans the whole Hubble sequence. The potential implications of the constancy of μ_0 are discussed in Donato et al. (2009).

In their modelling of spiral galaxies using the URC hypothesis, PSS found that the parameters of their Burkert DM haloes were correlated with those of the luminous matter. In Fig. 5 we show the ρ_0 versus R_D relationship for our dSph sample compared with the corresponding relation for spirals from PSS. As in the case of the ρ_0–r_0 relation in Fig. 2, the dSph data are consistent with the extrapolation of the relation seen in spirals. The significance of

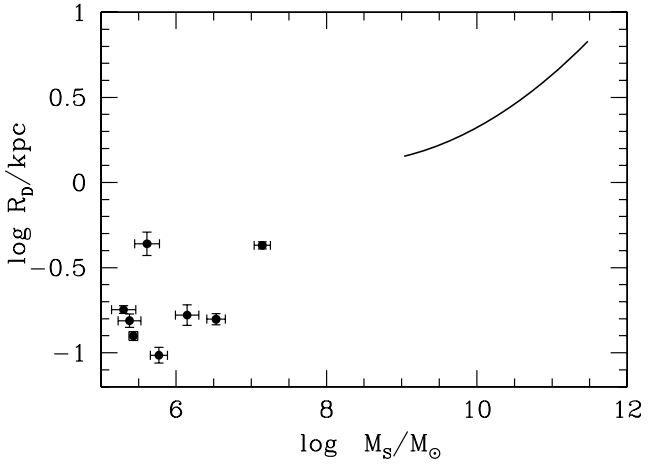

Figure 3. Comparison of the distribution of the characteristic baryonic scale R_D versus stellar mass M_s for dSphs (points; this paper) with the corresponding relation in spirals (from PSS). See Section 1 for the definition of R_D used for the dSph sample.

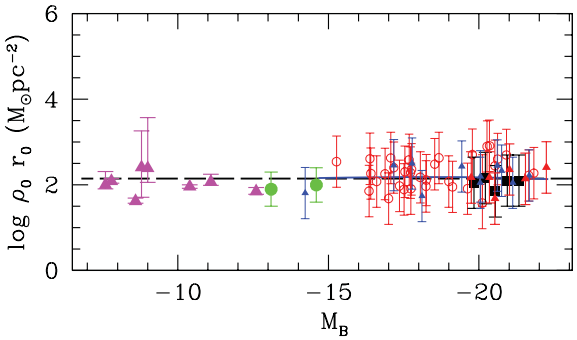

Figure 4. $\rho_0 r_0$ in units of $M_\odot$ pc^2 as a function of galaxy magnitude for different galaxies and Hubble types. The data are: (1) the Spano et al. (2008) sample of spiral galaxy data (open red circles); (2) the URC relation (solid blue line; Shankar et al. 2006); (3) the dwarf irregulars N3741 (M_B = 13.1; Gentile et al. 2007) and DDO 47 (M_B = 14.6; Gentile et al. 2005) (full green circles), spirals and ellipticals (black squares; Hoekstra et al. 2005) investigated by weak lensing; (4) Milky Way dSphs (pink triangles; this paper); (5) nearby spirals in the HI nearby galaxy survey (THINGS) (small blue triangles; Walter et al. 2008); and (6) early-type spirals (full red triangles; Noordermeer 2006; Noordermeer et al. 2007). The long-dashed line shows the Donato et al. (2009) result.

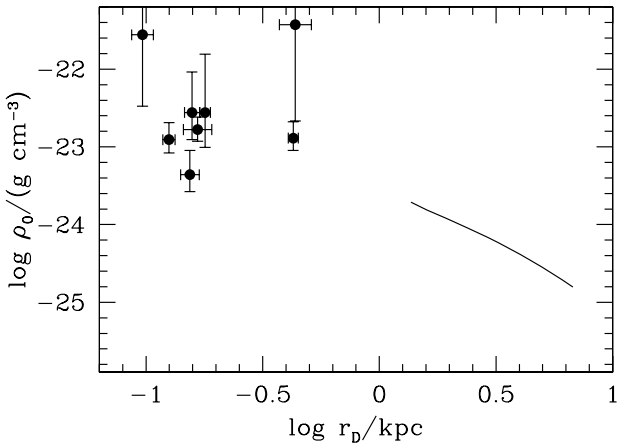

Figure 5. Halo central density ρ_0 versus stellar length-scale R_D for spirals (solid curve) and dSphs (points).

this relation derives from the fact that it links the DM and baryonic matter properties of galaxies on a wide range of length-scales: qualitatively, the 'central' densities of DM haloes increase as the extent of their associated stellar components decreases. Although the observational evidence for this relation is relatively strong, we stress that its physical interpretation is presently unknown (see Angus 2008; Gentile et al. 2009, for some related discussion of this point).

It is interesting to consider explicitly the role played by velocity anisotropy in this result. Unsurprisingly, under the assumption of Burkert haloes for dSphs, the inclusion of velocity anisotropy as a free parameter improves the quality of the dispersion profile fits relative to those obtained for isotropic models. However, we also find that the scatter in the ρ_0–r_0 relation is smaller for anisotropic models – thus the better we reproduce the observed dispersion profiles using Burkert haloes, the tighter is the correlation between the halo parameters.

Finally, we emphasize that the present results do not *require* the presence of cored haloes in dSphs, nor do they constrain the density and scalelengths of their haloes in a model-independent way. On the other hand, the fact that the dSph kinematics can be reproduced using Burkert DM halo profiles whose structural parameters lie on the same scaling relations as those of spirals provides some support for the claim that the mass distributions in dSph galaxies can be understood within the same framework as those of spirals.

4 CONCLUSIONS

Dwarf spheroidal galaxies are the lowest luminosity stellar systems which show evidence of dynamically significant DM. Their physical properties (luminosity, stellar scalelength and baryon fraction) are typically two orders of magnitude different from those observed for spiral and elliptical galaxies. Given these extreme structural properties, an understanding of the formation of dSphs is crucial for the development of a complete picture of galaxy formation.

The main result of this paper is the finding that these galaxies, despite being very distinct in their physical properties from spirals and ellipticals and having a large individual scatter in their baryonic properties, exhibit kinematic properties that can be modelled using DM haloes with the same mass profiles as those which reproduce the rotation curves of spiral galaxies. Under the assumption that the haloes of dSphs have Burkert profiles, we find that the derived central densities and the core radii are consistent with the extrapolation of the relationship between these quantities seen in spiral galaxies. Conversely, a Burkert profile with structural parameters predicted by the extrapolation of the relation between halo central density and DM core radius previously found from Burkert fits to the kinematics of elliptical and spiral galaxies can account for the observed internal kinematics in dSphs.

This result is intriguing, and could point to a common physical process responsible for the formation of cores in galactic haloes of all sizes, or to a strong coupling between the DM and luminous matter in dSphs. It is worth noting that a potential connection between spiral galaxies and dSphs does not appear as natural as one between dSphs and other hot, spheroidal systems (Dabringhausen, Hilker & Kroupa 2008; Forbes et al. 2008). For example, while the sizes of spiral galaxies are presumably fixed by the angular momentum of the gas from which they form, most of the present-day dSphs show no signs of rotation (although Battaglia et al. 2008 have recently found evidence of rotation in the Sculptor dSph). However, Mayer et al. (2001) have proposed a formation scenario for dSphs in which they are initially low-mass disc galaxies that are subsequently transformed into spheroids by tidal interaction with the Milky Way. More recently, such models have been shown to provide reasonable models for the properties of the Fornax (Klimentowski et al. 2007) and LeoI dSphs (Łokas et al. 2008). If the haloes of dSphs do indeed follow the scaling laws defined by more massive disc galaxies, this could lend indirect support to evolutionary histories of this kind. Suggestive evidence of such transformation scenarios is also provided by the discovery of residual discs with spiral structure in luminous dwarf elliptical galaxies in the Virgo cluster (Lisker, Grebel & Binggeli 2006).

Further dynamical analysis is needed to derive the actual DM distribution in dSph and possibly to estimate their halo core radii. Nevertheless, it interesting to speculate on the possible implications of these scaling laws for our understanding of DM. Warm DM has been invoked as a potential solution to the overprediction of substructure by Λ cold dark matter (ΛCDM) simulations, and to the cusp–core issue (e.g. Moore et al. 1999). However, the existence of scaling relations between the central density and core radius over three orders of magnitude in both quantities would argue against this explanation, unless the warm DM spectrum is extremely

fine-tuned. Furthermore, such DM relations cannot arise due to either self-annihilation or decay of DM, which would predict a narrow range in ρ_0 and no clear correlation of the latter with the core radius.

Dalcanton & Hogan (2001) argued that the phase-space densities of DM haloes suggested that warm DM (either collisional or collisionless) could not be the cause of cores in galaxy haloes on all scales. These authors suggested a dynamical origin for the cores of larger galaxies. Subsequently, a number of studies have demonstrated that macroscopic core formation in galaxy haloes is possible through the infall of compact baryonic (or baryon dominated) subclumps (El-Zant, Shlosman & Hoffman 2001; Jardel & Sellwood 2009; Goerdt et al. 2010; Cole, Dehnen & Wilkinson 2011). Further work is required to explore whether such processes, in conjunction with subsequent star formation and feedback (e.g. Pasetto et al. 2010), can result in universal scaling relations spanning three orders of magnitude in density and length-scales.

Clearly, a direct kinematic determination of the DM profiles of dSphs is essential to confirm the robustness of the scaling relations between the halo parameters. A number of recent papers have made progress towards this goal in the subset of dSphs which exhibit kinematically distinct subpopulations in their stellar components (Battaglia et al. 2008; Walker & Peñarrubia 2011; Amorisco & Evans 2012). Interestingly, all three analyses favour cored haloes over cusped ones. However, further observational and modelling work is required to constrain the halo profiles more tightly. Theoretically, the development of a physical picture of the processes which shape the halo profiles of dSphs and which could lead to the existence of apparently similar scaling relations between halo properties over a wide range of galaxy luminosities is an important research goal for the coming years.

ACKNOWLEDGMENTS

MIW acknowledges support from a Royal Society University Research Fellowship. MGW is supported by NASA through Hubble Fellowship grant HST-HF-51283.01-A, awarded by the Space Telescope Science Institute, which is operated by the Association of Universities for Research in Astronomy, Inc., for NASA, under contract NAS5-26555. EKG is supported by Sonderforschungsbereich SFB 881 'The Milky Way System' (subproject A2) of the German Research Foundation (DFG). AK thanks the Deutsche Forschungsgemeinschaft for funding from Emmy-Noether grant Ko 4161/1.

REFERENCES

Adén D., Wilkinson M. I., Read J. I., Feltzing S., Koch A., Gilmore G. F., Grebel E. K., Lundström I., 2009, ApJ, 706, L150
Amorisco N. C., Evans N. W., 2012, MNRAS, 419, 184
Angus G. W., 2008, MNRAS, 387, 1481
Ashman K. M., 1992, PASP, 104, 1109
Battaglia G., Helmi A., Tolstoy E., Irwin M., Hill V., Jablonka P., 2008, ApJ, 681, L13
Binney J., Tremaine S., 2008, Galactic Dynamics, 2nd edn. Princeton Univ. Press, Princeton, NJ
Burkert A., 1995, ApJ, 447, L25
Chemin L., de Blok W. J. G., Mamon G. A., 2011, AJ, 142, 109
Cole D. R., Dehnen W., Wilkinson M. I., 2011, MNRAS, 416, 1118
Collins M. L. M. et al., 2010, MNRAS, 407, 2411
Collins M. L. M. et al., 2011, MNRAS, 417, 1170
Dabringhausen J., Hilker M., Kroupa P., 2008, MNRAS, 386, 864
Dalcanton J. J., Hogan C. J., 2001, ApJ, 561, 35
de Blok W. J. G., 2005, ApJ, 634, 227
de Blok W. J. G., Bosma A., 2002, A&A, 385, 816
de Blok W. J. G., McGaugh S. S., Rubin V. C., 2001, AJ, 122, 2396
de Blok W. J. G., Walter F., Brinks E., Trachternach C., Oh S.-H., Kennicutt R. C., Jr, 2008, AJ, 136, 2648
Donato F., Gentile G., Salucci P., 2004, MNRAS, 353, L17
Donato F. et al., 2009, MNRAS, 397, 1169
El-Zant A., Shlosman I., Hoffman Y., 2001, ApJ, 560, 636
Evans N. W., An J., Walker M. G., 2009, MNRAS, 393, L50
Forbes D., Lasky P., Graham A., Spitler L., 2008, MNRAS, 389, 1924
Freeman K. C., 1970, ApJ, 160, 811
Gentile G., Salucci P., Klein U., Vergani D., Kalberla P., 2004, MNRAS, 351, 903
Gentile G., Burkert A., Salucci P., Klein U., Walter F., 2005, ApJ, 634, L145
Gentile G., Salucci P., Klein U., Granato G. L., 2007, MNRAS, 375, 199
Gentile G., Famaey B., Zhao H., Salucci P., 2009, Nat, 461, 627
Gilmore G., Wilkinson M. I., Wyse R. F. G., Kleyna J. T., Koch A., Evans N. W., Grebel E. K., 2007, ApJ, 663, 948
Goerdt T., Moore B., Read J. I., Stadel J., Zemp M., 2006, MNRAS, 368, 1073
Goerdt T., Moore B., Read J. I., Stadel J., 2010, ApJ, 725, 1707
Grebel E. K., Gallagher J. S. III, Harbeck D., 2003, AJ, 125, 1926
Hastings W. K., 1970, Biometrika, 57, 97
Helmi A., 2008, A&AR, 15, 145
Hoekstra H., Hsieh B. C., Yee H. K. C., Lin H., Gladders M. D., 2005, ApJ, 635, 73
Irwin M., Hatzidimitriou D., 1995, MNRAS, 277, 1354
Jardel J. R., Sellwood J. A., 2009, ApJ, 691, 1300
Kalirai J. S. et al., 2010, ApJ, 711, 671
Kleyna J., Wilkinson M. I., Evans N. W., Gilmore G., Frayn C., 2002, MNRAS, 330, 792
Kleyna J. T., Wilkinson M. I., Evans N. W., Gilmore G., 2004, MNRAS, 354, L66
Klimentowski J., Łokas E. L., Kazantzidis S., Prada F., Mayer L., Mamon G. A., 2007, MNRAS, 378, 353
Koch A., Wilkinson M. I., Kleyna J. T., Gilmore G. F., Grebel E. K., Mackey A. D., Evans N. W., Wyse R. F. G., 2007a, ApJ, 657, 241
Koch A., Kleyna J. T., Wilkinson M. I., Grebel E. K., Gilmore G. F., Evans N. W., Wyse R. F. G., Harbeck D. R., 2007b, AJ, 134, 566
Kormendy J., 1985, ApJ, 295, 73
Kormendy J., 1987, in Faber S. M., ed., Nearly Normal Galaxies: From the Planck Time to the Present. Springer-Verlag, New York, p. 163
Kormendy J., 1990, in Kron R. G., ed., Evolution of the Universe of Galaxies. · Astron. Soc. Pac., San Francisco, p. 33
Kormendy J., Freeman K. C., 2004, in Ryder S. D., Pisano D. J., Walker M. A., Freeman K. C., eds, IAU Symp., 220, Scaling Laws for Dark Matter Halos in Late-Type and Dwarf Spheroidal Galaxies. Astron. Soc. Pac., San Francisco, p. 377
Kuzio de Naray R., McGaugh S. S., de Blok W. J. G., Bosma A., 2006, ApJS, 165, 461
Lisker T., Grebel E. K., Binggeli B., 2006, AJ, 132, 497
Łokas E. L., Klimentowski J., Kazantzidis S., Mayer L., 2008, MNRAS, 390, 625
Mamon G. A., Łokas E. L., 2005, MNRAS, 363, 705
Marchesini D., D'Onghia E., Chincarini G., Firmani C., Conconi P., Molinari E., Zacchei A., 2002, ApJ, 575, 801
Martin N. F., de Jong J. T. A., Rix H.-W., 2008, ApJ, 684, 1075
Mateo M. L., 1998, ARA&A, 36, 435
Mateo M., Olszewski E. W., Vogt S. S., Keane M. J., 1998, AJ, 116, 2315
Mateo M. L., Olszewski E. W., Walker M. G., 2008, ApJ, 675, 201
Mayer L., Governato F., Colpi M., Moore B., Quinn T., Wadsley J., Stadel J., Lake G., 2001, ApJ, 559, 754
Metropolis A. W., Rosenbluth M. N., Teller A. H., Teller E., 1953, J. Chem. Phys., 21, 1087
Moore B., Quinn T., Governato F., Stadel J., Lake G., 1999, MNRAS, 310, 1147
Muñoz R. R. et al., 2005, ApJ, 631, L137
Muñoz R. R. et al., 2006, ApJ, 649, 201
Napolitano N. R., Romanowsky A. J., Tortora C., 2010, MNRAS, 405, 2351

Navarro J. F., Frenk C. S., White S. D. M., 1997, ApJ, 490, 493
Noordermeer E., 2006, PhD thesis, Rijksuniversiteit, Groningen
Noordermeer E., van der Hulst J. M., Sancisi R., Swaters R. S., van Albada T. S., 2007, MNRAS, 376, 1513
Pasetto S., Grebel E. K., Berczik P., Spurzem R., Dehnen W., 2010, A&A, 514, A47
Peñarrubia J., McConnachie A. W., Navarro J. F., 2008, ApJ, 672, 904
Persic M., Salucci P., 1988, MNRAS, 234, 131
Persic M., Salucci P., 1991, ApJ, 368, 60
Persic M., Salucci P., Stel F., 1996, MNRAS, 281, 27 (PSS)
Plummer H. C., 1915, MNRAS, 76, 107
Salucci P., Burkert A., 2000, ApJ, 537, L9
Salucci P., Lapi A., Tonini C., Gentile G., Yegorova I., Klein U., 2007, MNRAS, 378, 41
Shankar F., Lapi A., Salucci P., De Zotti G., Danese L., 2006, ApJ, 643, 14
Sofue Y., Rubin V., 2001, ARA&A, 39, 137
Spano M., Marcelin M., Amram P., Carignan C., Epinat B., Hernandez O., 2008, MNRAS, 383, 297
Strigari L. E., Bullock J. S., Kaplinghat M., Simon J. D., Geha M., Willman B., Walker M. G., 2008, Nat, 454, 1096
Tolstoy E. et al., 2004, ApJ, 617, L119
Walker M. G., Peñarrubia J., 2011, ApJ, 742, 20
Walker M. G., Mateo M., Olszewski E. W., Gnedin O. Y., Wang X., Sen B., Woodroofe M., 2007, ApJ, 667, L53
Walker M. G., Mateo M., Olszewski E. W., 2009a, AJ, 137, 2100
Walker M. G., Mateo M., Olszewski E. W., Peñarrubia J., Wyn Evans N., Gilmore G., 2009b, ApJ, 704, 1274
Walker M. G., Mateo M., Olszewski E. W., Peñarrubia J., Wyn Evans N., Gilmore G., 2010, ApJ, 710, 886
Walter F., Brinks E., de Blok W. J. G., Bigiel F., Kennicutt R. C., Jr, Thornley M. D., Leroy A., 2008, AJ, 136, 2563
Wilkinson M. I., Kleyna J. T., Evans N. W., Gilmore G. F., Irwin M. J., Grebel E. K., 2004, ApJ, 611, L21

This paper has been typeset from a TEX/LATEX file prepared by the author.